Homogeneous Catalysis

Deutsche Ausgabe: DOI: 10.1002/ange.201607460
Internationale Ausgabe: DOI: 10.1002/anie.201607460

Controlling Proton Delivery through Catalyst Structural Dynamics

*Allan Jay P. Cardenas, Bojana Ginovska, Neeraj Kumar, Jianbo Hou, Simone Raugei, Monte L. Helm, Aaron M. Appel, R. Morris Bullock, and Molly O'Hagan**

Abstract: *The fastest synthetic molecular catalysts for H_2 production and oxidation emulate components of the active site of hydrogenases. The critical role of controlled structural dynamics is recognized for many enzymes, including hydrogenases, but is largely neglected in designing synthetic catalysts. Our results demonstrate the impact of controlling structural dynamics on H_2 production rates for $[Ni(P^{Ph}{}_2N^{C6H4R}{}_2)_2]^{2+}$ catalysts (R = n-hexyl, n-decyl, n-tetradecyl, n-octadecyl, phenyl, or cyclohexyl). The turnover frequencies correlate inversely with the rates of chair–boat ring inversion of the ligand, since this dynamic process governs protonation at either catalytically productive or non-productive sites. These results demonstrate that the dynamic processes involved in proton delivery can be controlled through modification of the outer coordination sphere, in a manner similar to the role of the protein architecture in many enzymes. As a design parameter, controlling structural dynamics can increase H_2 production rates by three orders of magnitude with a minimal increase in overpotential.*

The high catalytic efficiency of metalloenzymes is attributed to the active-site structure and control of the active-site environment, including the precise regulation of substrate delivery and product removal. This regulation is achieved through the extended architecture of the protein, interaction with the medium, and controlled structural dynamics, which can dictate active-site access as well as precise positioning of active components throughout the catalytic reaction.[1] The structural dynamics of molecular catalysts can also have a profound effect on catalytic performance. Dynamics has been used as a design feature to modulate chemoselectivity and enantioselectivity,[2] to enhance electron transfer,[3] to determine enantiomeric excess,[4] and even to turn the activity of the catalyst on or off.[5] However, predicting and controlling the effects that ligand dynamic processes can have on reactivity is challenging when designing new catalytic systems, whether synthetic molecular systems or within a protein framework. In this study, the importance of controlling structural dynamics in catalysis is demonstrated through the modulation of catalytic rates over three orders of magnitude for molecular Ni electrocatalysts for H_2 production. This rate enhancement is achieved by controlling the structural dynamics involved in key proton-transfer steps.

Highly active electrocatalysts for the production and oxidation of H_2, such as the $[Ni(P^R{}_2N^{R'}{}_2)_2]^{2+}$ catalysts ($P^R{}_2N^{R'}{}_2$ = 1,5-diaza-3,7-diphosphacyclooctane with alkyl or aryl groups on the P and N atoms), have been developed by incorporating a base in the second coordination sphere of the metal to act as a proton relay (Scheme 1), a system similar to the active site of the [FeFe]-hydrogenase.[6] The reactivity of

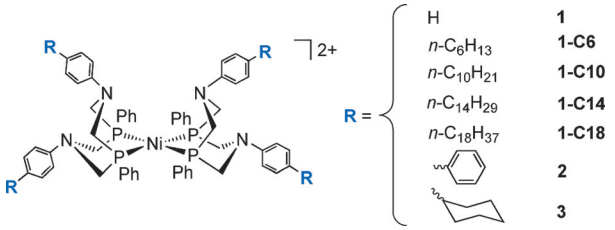

Scheme 1. Structure of the nickel(II) complexes: $[Ni(P^{Ph}{}_2N^{C6H4R}{}_2)_2]^{2+}$. For complex characterization, including X-ray structures, see the the Supporting Information.

these modular catalysts can be controlled through systematic changes in the steric and electronic characteristics of the ligands and the basicity of the pendant amine.[7] Changes to the medium composition have substantial effects on the reactivity of these complexes, with significant rate enhancements observed in protic ionic liquid/H_2O media compared to traditional organic solvents.[8] Proton mobility in these media is critical for fast catalysis, but proton mobility alone does not account for the observed rate enhancement, especially for **1-C6**.[8b] We have now identified the source of the dramatic rate enhancement as modulation of the ligand dynamics that control the positioning of the pendant amine, and therefore the protonation site. We observed a remarkable correlation between ligand structural dynamics and catalytic performance, which is controlled through different substituents on the periphery of the ligand, seven bonds away from the metal (Scheme 1). Controlling the ligand dynamics led to an increase in the catalytic activity by more than three orders of magnitude in acetonitrile/water solution, giving H_2 production turnover frequencies of $1.5 \times 10^6\ s^{-1}$. By combining catalyst modification and the use of protic ionic liquids, we achieved catalytic rates up to $4.5 \times 10^7\ s^{-1}$, which, to our knowledge, is the fastest catalysis for this transformation to date.

[*] Dr. A. J. P. Cardenas, B. Ginovska, Dr. N. Kumar, Dr. J. Hou, Dr. S. Raugei, Dr. M. L. Helm, Dr. A. M. Appel, Dr. R. M. Bullock, Dr. M. O'Hagan
Center for Molecular Electrocatalysis
Pacific Northwest National Laboratory
P.O. Box 999, K2-57, Richland, WA 99352 (USA)
E-mail: molly.ohagan@pnnl.com
Dr. A. J. P. Cardenas
Current address: 221 Science Center
State University of New York at Fredonia
Fredonia, NY 14063 (USA)

Supporting information for this article can be found under: http://dx.doi.org/10.1002/anie.201607460.

To rapidly reduce protons, the six-membered ring containing the pendant amine and the metal center of $[Ni(P^{R}_{2}N^{R'}_{2})_2]^{2+}$ systems must adopt a boat conformation (Scheme 2), with the lone pair of the amine oriented *endo*

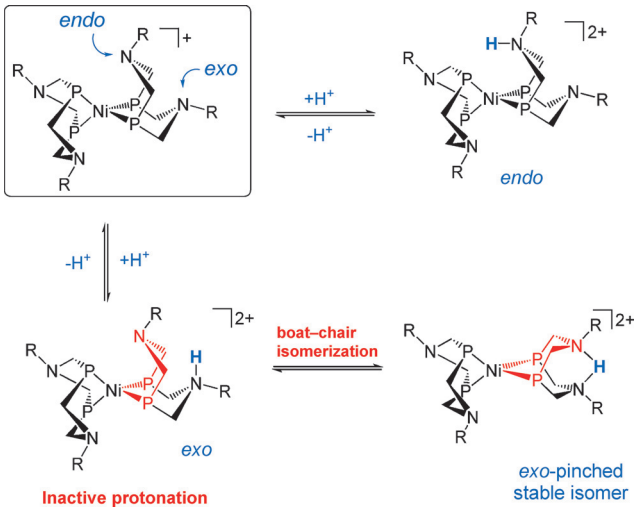

Scheme 2. Branching of the catalytic cycle occurs due to protonation at the inactive *exo* site or active *endo* site. Only *endo* protonation results in H_2 formation (top pathway). The *exo* protonation is stabilized by boat-to-chair isomerization of the ligand to form a hydrogen bond (bottom pathway), thereby resulting in a conformer that is thermodynamically and kinetically stabilized to the deprotonation required to resume catalytic activity.

with respect to the metal center. Protonation of the chair conformer, which is often the kinetically preferred protonation site, positions protons *exo* to the metal center, where they cannot interact with the metal center. To produce H_2, these *exo*-protonated species require isomerization through deprotonation of the *exo* position followed by protonation in the *endo* position. This isomerization process is slow relative to electrocatalysis, and leads to accumulation of the *exo*-protonated species in the electrochemical diffusion layer, effectively attenuating the concentration of the active catalyst and thereby decreasing the observed rates of catalysis.[7a,9] The stability of the *exo*-protonated isomers is increased by intramolecular N–H···N hydrogen bonding, that is, the "*exo* pinch", which stabilizes the protonation site by more than 5 pK_a units relative to the non-pinched isomer.[10] The kinetic stability of the protonation site is also increased by the presence of the hydrogen-bonding interaction, where access to the *exo*-pinched proton by the external base is hindered by the second amine. Avoiding the formation of the N–H···N hydrogen bond would greatly accelerate the *exo–endo* isomerization process and therefore the rate of catalysis. The formation of the *exo*-pinched species could be limited by slowing the boat–chair isomerization that leads to the pinched species, as illustrated in Scheme 2. To test this hypothesis, we synthesized a series of catalyst derivatives with various substituents in the outer coordination sphere, and measured the impact of slowed structural dynamics on catalytic performance.

In many natural catalysts, the outer coordination sphere modulates dynamic processes essential to catalysis through complex intramolecular and solvent interactions.[1] To emulate this control in a molecular system that is more synthetically accessible, substituents of varying size and structure were incorporated into the outer coordination sphere of the catalyst (Scheme 1) to modulate interconversion of the boat and chair conformers. The boat–chair isomerization rates for the $[Ni(P^{Ph}_{2}N^{C6H4R}_{2})_2]^{2+}$ series of catalysts were measured by lineshape analysis of the variable-temperature $^{31}P\{^{1}H\}$ NMR spectra for the Ni^{II} complexes in CD_2Cl_2/CD_3CN as the solvent to provide the required low-temperature range for Eyring analysis.[11] The Ni^{II} complexes have a trigonal bipyramidal structure in which acetonitrile is the fifth ligand. The presence of this fifth ligand results in two different phosphorus environments in the trigonal bipyramidal structure, which interconvert through dissociation of the acetonitrile, chair–boat isomerization, and re-coordination of acetonitrile.[11] Details of the exchange process, representative spectra, and Eyring analyses are shown in the Supporting Information. As the length of the *n*-alkyl chain of the substituent in the outer coordination sphere is increased, the rate of chair–boat isomerization decreases, and the turnover frequency (TOF) increases up to three orders of magnitude, as shown in Figure 1. The $[Ni(P^{Ph}_{2}N^{C6H4R}_{2})_2]^{2+}$ complexes catalyze H_2

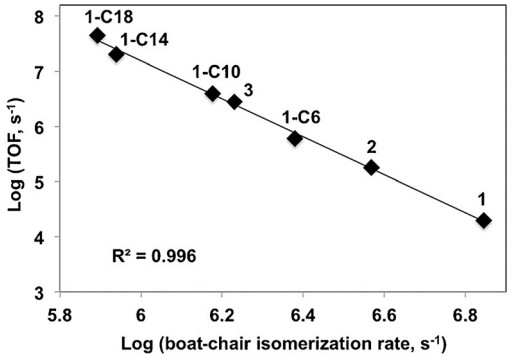

Figure 1. Correlation between catalytic rates of H_2 production measured in protonated dibutyl formamide bis(trifluoromethanesulfonyl)amide/water ([(DBF)H]NTf_2/H_2O) and boat–chair isomerization rates measured in 4:1 CD_2Cl_2/CD_3CN for the $[Ni(P^{Ph}_{2}N^{C6H4R}_{2})_2]^{2+}$ series.

production, and the plateau of the scan-rate-independent electrocatalytic current was used to determine the catalytic rate, or TOF, in the media indicated in Table 1 by using established methods.[12] For each catalyst, the catalytic current (i_{cat}) exhibited first-order dependence on catalyst concentration and plateaued to the steady-state value as the scan rate, acid concentration, and water content increased (Figures S4–S9 in the Supporting Information). A strong linear correlation is observed between the log(TOF) vs. log(boat–chair isomerization rate) values for the seven complexes of the series in three media, which is consistent with the dependence of the TOF on the boat–chair isomerization rates. Complexes **2** and **3** exhibit TOFs that fit the linear correlation. Notably, the TOF does not correlate with the structure of the outer-coordination-sphere substituents or the driving force for

Table 1: Boat–chair isomerization rates, turnover frequencies, and overpotentials of the $[Ni(P^{Ph}_2N^{C6H4R}_2)_2]^{2+}$ series.

$[Ni(P^{Ph}_2N^{C6H4R}_2)_2]^{2+}$	Boat–chair isomerization rates	MeCN Dry		MeCN Wet (0.8–1.1 M H_2O)		$[(DBF)H]NTf_2/H_2O$ $\chi_{H_2O}=0.68$–0.71	
	[a] k_{298K} [s^{-1}]	TOF [s^{-1}]	η [mV]	TOF [s^{-1}]	η [mV]	TOF [s^{-1}]	η [mV]
1	7.0×10^6	590	400	720	400	6.0×10^4	420
1-C6	2.4×10^6	200	340	740	400	6.0×10^5	410
1-C10	1.5×10^6	740	310	3400	420	4.0×10^6	440
1-C14	8.7×10^5	2900	320	9.8×10^4	440	2.0×10^7	520
1-C18	7.5×10^5	2.9×10^4	330	1.5×10^6	470	$\approx4.5\times10^7$ [b]	570
2	3.7×10^6	690	330	4000	440	1.8×10^5	430
3	1.7×10^6	400	370	1500	470	2.5×10^6	500

[a] Boat–chair isomerization rates measured in 4:1 CD_2Cl_2:CD_3CN. With the addition of water, up to 0.5 M, no change in the boat–chair isomerization rates were observed compared to dry solvents. [b] Due to limited solubility in $[(DBF)H]NTf_2/H_2O$, the diffusion coefficients for **1-C18** could not be measured. Therefore, the TOF of **1-C18** was estimated using the D_{cat} measured for **1-C14**.

protonation and H_2 formation, that is, the basicity of the pendant amine and metal center.[7a]

Recent kinetic analysis of $[Ni(P^R_2N^{R'}_2)_2]^{2+}$ systems identifies proton transfer, that is, protonation/deprotonation, as a limiting factor for catalysis, and illustrates that the addition of water reduces these barriers, thereby increasing catalytic rates.[13] In comparing the alkyl series **1-C6** through **1-C18**, a TOF increase of 150-fold is observed in dry MeCN as the boat–chair isomerization rate is decreased by a factor of nine. In MeCN with added water, a 2000-fold faster rate is observed for **1-C18** compared to **1-C6**, with no additional change in boat–chair isomerization rate (Figure 2). These data suggest that in dry acetonitrile, protonation/deprotonation is competitive with boat–chair isomerization for the rate-determining step(s), but not when water is added to facilitate proton transfer. If proton delivery or removal is no longer rate-limiting, the boat–chair inversion process controls catalysis by attenuating the formation of the catalytically incompetent *exo*-pinched isomer.[9] A detailed mechanistic understanding of this system has guided catalyst design and medium selection to control proton delivery and thereby attain fast rates. Further rate enhancement for this series, up to $4.5\times10^7\ s^{-1}$, is observed in $[(DBF)H]NTf_2/H_2O$ (Figure 2), thus indicating that this medium affords rapid proton movement[8b] and possibly further attenuation of the structural dynamics due to solvent effects such as viscosity,[14] hydrophobicity, or ion pairing (Table S5).

In addition to slowing ligand structural dynamics, the long alkyl chain may facilitate fast rates by sterically blocking the *exo* protonation site through hydrophobic packing, either intra- or intermolecularly. As shown in the crystal structures of the Ni^0 complexes (Figure S16), the alkyl chains of the Ni^0 complex **1-C14**, that is, **1-C14a**, do stack intermolecularly in an extended structure, with similar structural motifs observed for both **1-C10a** and **1-C6a**. Such intermolecular aggregation has been hypothesized to enhance catalytic rates in molecular catalysts such as the iridium water-oxidation catalysts reported by Macchioni and co-workers.[15] In the case of the **1-Cn** series reported here, increasing the alkyl chain length does not substantially affect the diffusion coefficients (Table S1). The difference between the diffusion coefficients of these catalysts and other catalysts with *para* substituents, such as Br or OMe,[8b] is small and may be accounted for by their increased size. The relative diffusion coefficients are not consistent with aggregation of the catalysts in solution. Furthermore, the diffusion coefficients are not concentration

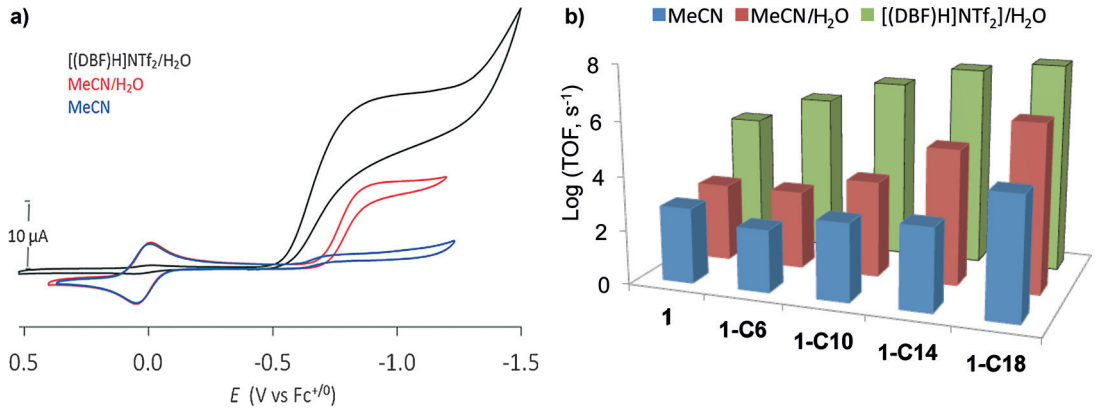

Figure 2. a) Cyclic voltammogram of 10 μM **1-C14** in acetonitrile (MeCN; blue); and MeCN with 1.1 M water (MeCN/H_2O; red); with 0.2 M Bu_4NBF_4 supporting electrolyte and using 600 mM protonated dimethyl formamide $[(DMF)H^+]$ as the acid. The black trace is the cyclic voltammogram of 10 μM **1-C14** in $[(DBF)H]NTf_2/H_2O$, $\chi_{H_2O}=0.68$. Conditions: scan rate of 0.2 Vs^{-1}, 1 mm glassy carbon working electrode, potentials referenced to $Cp_2Fe^{+/0}$ (0 V). b) Comparison of TOF for the $[Ni(P^{Ph}_2N^{C6H4R}_2)_2]^{2+}$ series in three media listed in (a).

dependent (Table S6), and the catalytic current shows first-order dependence on catalyst concentration (Figure S7). These findings are not consistent with the rate of enhancement being the result of oligomerization. Modulation of the structural dynamics by intramolecular interactions, as well as the potential impact of solvent upon intramolecular interactions, was investigated computationally and is discussed in the Supporting Information.

The TOF increases up to three orders of magnitude while the rate of isomerization decreases by approximately one order of magnitude, that is, an increase in $\Delta G^{\ddagger}_{\text{isomerization}}$ of 1.4 kcal mol^{-1}. A larger change in $\Delta G^{\ddagger}$ would be expected given that the barrier is proposed to be the key contributor to the change in the catalytic rates. However, the barrier for the isomerization process could only be measured for the Ni^{II} complexes as a model for the reduced nickel complexes that are protonated during catalysis. The trend measured for the Ni^{II} series, that is, decreasing isomerization rates with increased substituent size, is expected to be maintained for all oxidation states of the metal center[11] and medium compositions (Table S5). Moreover, the effect that the change in isomerization barrier has on the catalytic rate is expected to be compounded by the presence of two required proton transfers for the production of H_2, both of which are complicated by multiple possible protonation sites.[9]

The large increase in TOF observed for these systems is not accompanied by a substantial increase in overpotential (Figure 3). The overpotential was experimentally determined

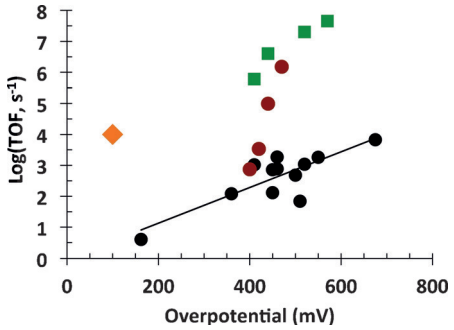

Figure 3. The Log TOF is plotted as a function of overpotential for the [FeFe]-hydrogenase (orange diamond),[6,17] the $[Ni(P^{R}_{2}N^{R'}_{2})_2]^{2+}$ family with varying R, R′ groups (black circles),[18] and the $[Ni(P^{Ph}_{2}N^{C6H4R}_{2})_2]^{2+}$ series (red circles) in MeCN/H_2O with 0.2 M Bu_4NBF_4 supporting electrolyte and (DMF)H^+ as the acid; and the $[Ni(P^{Ph}_{2}N^{C6H4R}_{2})_2]^{2+}$ series in [(DBF)H]NTf_2/H_2O (green squares).

from the difference between the observed potential for catalysis ($E_{cat/2}$) and the thermodynamic potential measured in the three different media using the open-circuit potential measurements, with solvent conditions identical to the catalysis experiments.[16] In MeCN/H_2O medium, the TOF of **1-C18** is three orders of magnitude faster than that of **1-C6**, with only a 70 mV increase in overpotential.

Many enzymes use restricted structural dynamics around the active site to optimize reactivity by controlling substrate delivery.[1d] In the [FeFe]-hydrogenase active site, precise positioning of the proton relay *endo* to the Fe site with the open coordination site is necessary for accepting/delivering protons, and this is achieved through interactions with the outer coordination sphere.[6b] Extensive control of the ligand structural dynamics in the $[Ni(P^{Ph}_{2}N^{C6H4R}_{2})_2]^{2+}$ system can be attained through modifications to the outer coordination sphere that result in mesoscale medium effects. By including control of ligand structural dynamics as a design feature of molecular catalysts, the rates of H_2 production by the $[Ni(P^{Ph}_{2}N^{C6H4R}_{2})_2]^{2+}$ system are enhanced by three orders of magnitude without a significant loss in energy efficiency. The remarkable rate enhancements observed in the $[Ni(P^{Ph}_{2}N^{C6H4R}_{2})_2]^{2+}$ system as a function of controlled structural dynamics illustrate how this new design parameter can be used to obtain catalytic performance that rivals that of enzymes.

Acknowledgements

This research was supported as part of the Center for Molecular Electrocatalysis, an Energy Frontier Research Center funded by the U.S. Department of Energy, Office of Science, Office of Basic Energy Sciences, and was performed in part using the Molecular Science Computing Facility in the William R. Wiley Environmental Molecular Sciences Laboratory, a DOE national scientific user facility located at the Pacific Northwest National Laboratory (PNNL). PNNL is operated by Battelle for DOE.

Keywords: artificial enzymes · electrocatalysis · homogeneous catalysis · hydrogen production · structural dynamics

How to cite: *Angew. Chem. Int. Ed.* **2016**, *55*, 13509–13513
Angew. Chem. **2016**, *128*, 13707–13711

[1] a) S. W. Ragsdale, *Chem. Rev.* **2006**, *106*, 3317–3337; b) G. Bhabha, J. T. Biel, J. S. Fraser, *Acc. Chem. Res.* **2015**, *48*, 423–430; c) J. P. Klinman, *Acc. Chem. Res.* **2015**, *48*, 449–456; d) G. G. Hammes, S. J. Benkovic, S. Hammes-Schiffer, *Biochemistry* **2011**, *50*, 10422–10430.
[2] a) N. Schneider, F. Schaper, K. Schmidt, R. Kirsten, A. Geyer, H. H. Brintzinger, *Organometallics* **2000**, *19*, 3597–3604; b) A. Nojiri, N. Kumagai, M. Shibasaki, *J. Am. Chem. Soc.* **2009**, *131*, 3779–3784.
[3] L. E. Sinks, M. R. Wasielewski, *J. Phys. Chem.* **2003**, *107*, 611–620.
[4] K. W. Bentley, C. Wolf, *J. Org. Chem.* **2014**, *79*, 6517–6531.
[5] R. Stoll, M. V. Peters, A. Kuhn, S. Heiles, R. Goddard, M. Buhl, C. M. Theile, S. Hecht, *J. Am. Chem. Soc.* **2009**, *131*, 357–367.
[6] a) J. C. Fontecilla-Camps, A. Volbeda, C. Cavazza, Y. Nicolet, *Chem. Rev.* **2007**, *107*, 4273–4303; b) J. W. Peters, W. N. Lanzilotta, B. J. Lemon, L. C. Seefeldt, *Science* **1998**, *282*, 1853–1858; c) W. Lubitz, H. Ogata, O. Rüdiger, E. Reijerse, *Chem. Rev.* **2014**, *114*, 4081–4148.
[7] a) D. L. DuBois, *Inorg. Chem.* **2014**, *53*, 3935–3960; b) R. M. Bullock, A. M. Appel, M. L. Helm, *Chem. Commun.* **2014**, *50*, 3125–3143.
[8] a) D. H. Pool, M. P. Stewart, M. O'Hagan, W. J. Shaw, J. A. S. Roberts, R. M. Bullock, D. L. DuBois, *Proc. Natl. Acad. Sci. USA* **2012**, *109*, 15634–15639; b) J. Hou, M. Fang, A. J. P.

Cardenas, W. J. Shaw, M. L. Helm, R. M. Bullock, J. A. Roberts, M. O'Hagan, *Energy Environ. Sci.* **2014**, *7*, 4013 – 4017.
[9] M.-H. Ho, R. Rousseau, J. A. S. Roberts, E. S. Wiedner, M. Dupuis, D. L. DuBois, R. M. Bullock, S. Raugei, *ACS Catal.* **2015**, *5*, 5436 – 5452.
[10] M. P. Stewart, M.-H. Ho, S. Wiese, M. L. Lindstrom, C. E. Thogerson, S. Raugei, R. M. Bullock, M. L. Helm, *J. Am. Chem. Soc.* **2013**, *135*, 6033 – 6046.
[11] J. A. Franz, M. O'Hagan, M.-H. Ho, T. Liu, M. L. Helm, S. Lense, D. L. DuBois, W. J. Shaw, A. M. Appel, S. Raugei, R. M. Bullock, *Organometallics* **2013**, *32*, 7034 – 7042.
[12] a) C. Costentin, J.-M. Savéant, *ChemElectroChem* **2014**, *1*, 1226 – 1236; b) J. M. Savéant, E. Vianello, *Electrochim. Acta* **1965**, *10*, 905 – 920.
[13] M.-H. Ho, M. O'Hagan, M. Dupuis, D. L. DuBois, R. M. Bullock, W. J. Shaw, S. Raugei, *Dalton Trans.* **2015**, *44*, 10969 – 10979.
[14] J. T. Barry, D. J. Berg, D. R. Tyler, *J. Am. Chem. Soc.* **2016**, *138*, 9389 – 9392.
[15] I. Corbucci, A. Petronilho, H. Muller-Bunz, E. Rocchigiani, M. Albrecht, A. Macchioni, *ACS Catal.* **2015**, *5*, 2714 – 2718.
[16] J. A. S. Roberts, R. M. Bullock, *Inorg. Chem.* **2013**, *52*, 3823 – 3835.
[17] C. Madden, M. D. Vaughn, I. Díez-Pérez, K. A. Brown, P. W. King, D. Gust, A. L. Moore, T. A. Moore, *J. Am. Chem. Soc.* **2012**, *134*, 1577 – 1582.
[18] a) U. Kilgore, J. Roberts, D. H. Pool, A. Appel, M. Stewart, M. Rakowski DuBois, W. G. Dougherty, W. S. Kassel, R. M. Bullock, D. L. DuBois, *J. Am. Chem. Soc.* **2011**, *133*, 5861 – 5872; b) U. J. Kilgore, M. P. Stewart, M. L. Helm, W. G. Dougherty, W. S. Kassel, M. R. DuBois, D. L. DuBois, R. M. Bullock, *Inorg. Chem.* **2011**, *50*, 10908 – 10918; c) S. Wiese, U. J. Kilgore, D. L. DuBois, R. M. Bullock, *ACS Catal.* **2012**, *2*, 720 – 727.

Received: August 2, 2016
Published online: September 27, 2016

